# Modelling the Milky Way Galaxy & the Large Magellanic Cloud

Introduction

## 1 Introduction

In this section some common quantities useful for describe the density profiles are defined and explained.

### 1.1 Critical density of the Universe:

The Critical density of the universe is defined as:

$$\rho_c = \frac{3H^2}{8\pi G} \tag{1}$$

Where $H$ is the Hubble parameter and this parameter depends on the cosmological parameters. This density ...

### 1.2 Virialization

A dark matter halo is virialized when it is in equilibrium, such an equilibrium occurs after the dark matter have collapsed and the force of gravity equals the **relaxation** processes [Binney and Tremaine, 2008]. This happens when the dark matter reach an overdensity value $\Delta_{vir}$. This overdensity corresponds to a radius and a mass $r_{vir}$ & $M_{vir}$ respectively.

$\Delta_{vir} = \frac{\rho_{vir}}{\rho_c}$. For a cosmolgy with $(\Omega_m + \Omega_\Lambda = 1)$ the solution for the **Top Hat** model can be approximated by:

$$\Delta_{vir} = (18\pi^2 + 82x - 39x^2)/\Omega(z) \tag{2}$$

[Eke et al., 1996, Bryan and Norman, 1998] Where $x = \Omega(z) - 1$. For the present time $(z = 0)$ $\Delta_{vir} = 360$.

The behavior of this function is shown in Fig.??

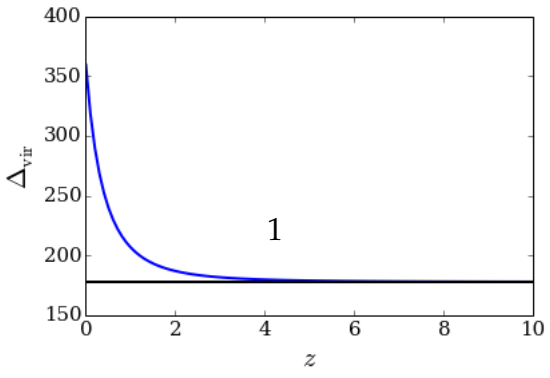

## 1.3 $r_{200}$ & $M_{200}$

There is another radious and mass of particular interest. This is the radius that enclosed a density of 200 times the density of the Universe. $M_{200}$ is defined as:

$$M_{200} = 200\rho_c \frac{4}{3}\pi r_{200}^3 \tag{5}$$

In the same way $M_{vir}$ is defined as:

$$M_{vir} = \Delta_{vir}\Omega_m \rho_c \frac{4}{3}\pi r_{vir}^3 \tag{6}$$

The critial density $\rho_c$ is the same for both cases, then it is possible to relate both masses from Eq5 and Eq6 as follows:

$$\frac{M_{200}}{M_{vir}} = \left(\frac{200}{\Delta_{vir}\Omega_m}\right)\left(\frac{r_{200}}{r_{vir}}\right)^3 \tag{7}$$

Here is common to call $q = \left(\frac{200}{\Delta_{vir}\Omega_m}\right)$, at $z = 0$ $q = 2.053$.

$$\frac{M_{200}}{M_{vir}} = q\left(\frac{r_{200}}{r_{vir}}\right)^3 \tag{8}$$

This Eq.8 relates $M_{vir}$ and $M_{200}$ for a given $rvir$ and $r_{200}$.

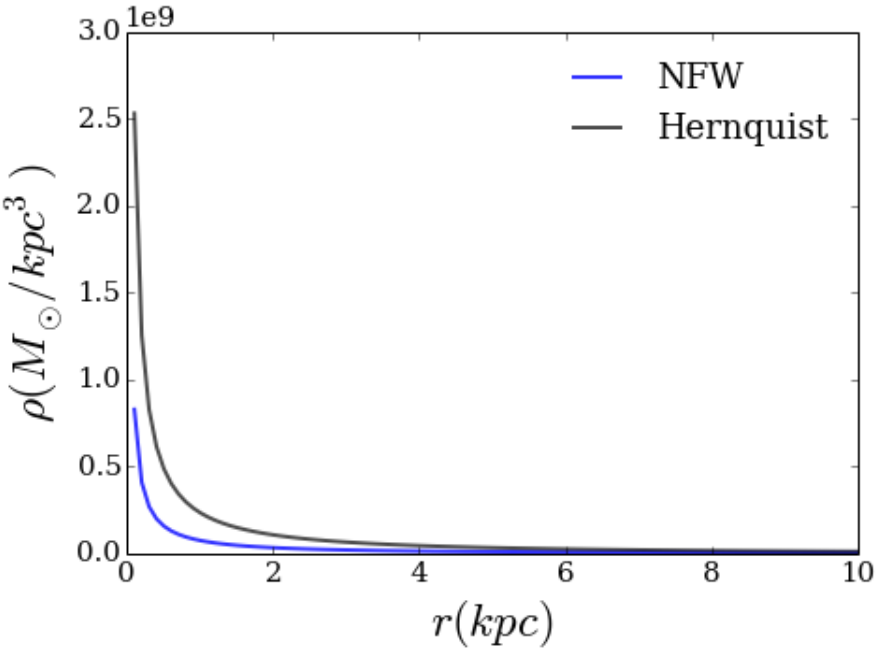


Spherical

# 2 Spherical Potentials

## 2.1 Plummer

The plumer density profile is one of the simplest models which describes a constant density near the center and falls at large radius.

$$\Phi_P(r) = -\frac{GM}{\sqrt{r^2 + a^2}} \tag{9}$$

Where $a$ is call the scale length. The scale length set the length $a$ in which the mayority of the density is enclosed. Note that if $a$ is cero the plummer potential would be exactly as the potential of a point mass. In the other hand if $a$ goes to infinity the potential is represents a very extended mass source. In other words the scale length set up the size of the volume in which the mass $M$ is enclosed.

Making use of the Poisson's equation one can derive the density from the potential and vice versa.

$$\nabla^2\Phi_P(r) = 4\pi G\rho_P(r) = \frac{1}{r^2}\frac{d}{dr}\left(r^2\frac{d\Phi_P(r)}{dr}\right) \tag{10}$$

$$\rho_P(r) = \frac{3M}{4\pi a^3}(1 + \frac{r^2}{a^2})^{-5/2} \tag{11}$$

The enclosed mass can be derived from the density by integrating over a volume or radius r.

$$M_P(< r) = 4\pi\int_0^r r'^2\frac{3M}{4\pi a^3}(1 + \frac{r'^2}{a^2})^{-5/2}dr' = \frac{3M}{a^3}\left(\frac{a^4r^3\sqrt{r^2/a^2 + 1}}{3(r^2 + a^2)^2}\right) \tag{12}$$

Making some algebra the total mass enclosed in radius $r$ is given by:

$$M_P(< r) = M\frac{r^3}{(a^2 + r^2)^{3/2}} \tag{13}$$

The cirular velocity can be derived from the total enclosed mass as follows:

$$v_c = \sqrt{\frac{GM(< r)}{r}} \tag{14}$$

$$v_c = \sqrt{GM\left(\frac{r^2}{(r^2 + a^2)^{3/2}}\right)} \tag{15}$$

Finally the acceleration can be derived using:

$$a = -\nabla\Phi \tag{16}$$

$$a = -\frac{GMr}{(r^2 + a^2)^{3/2}} \tag{17}$$

All this quantities are plotted in Fig.??.

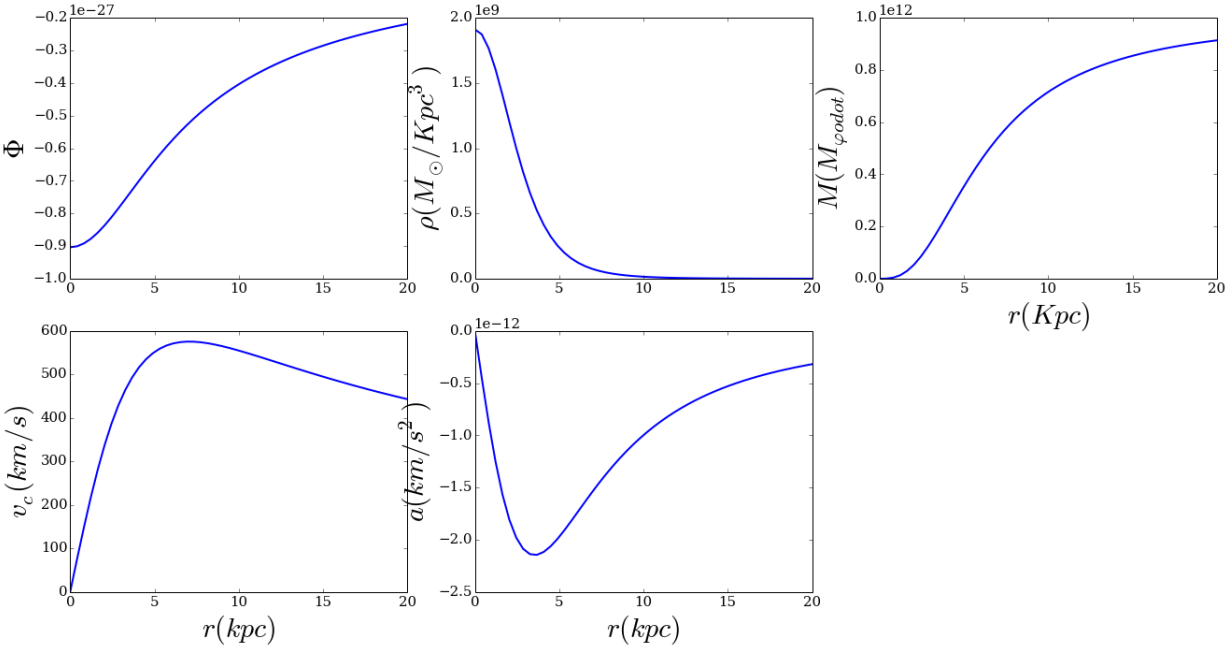


??

## 2.2 Hernquist profile

The Hernquist profile is derived in such a way that it follows the

$$\rho_{Hernquist}(r) = \frac{M}{2\pi}\frac{a}{r(r+a)^3} \tag{18}$$

$$M_{Hernquist}(< r) = 2aM\int \frac{r}{(r+a)^3}dr \tag{19}$$

$$M_{Hernquist}(< r) = M\frac{r^2}{(r+a)^2} \tag{20}$$

$$\Phi = -\frac{GM}{r+a} \tag{21}$$

$$v_c(r) = GM\frac{r}{(r+a)^2} \tag{22}$$

$$a = -\frac{GM}{(r+a)^2} \tag{23}$$

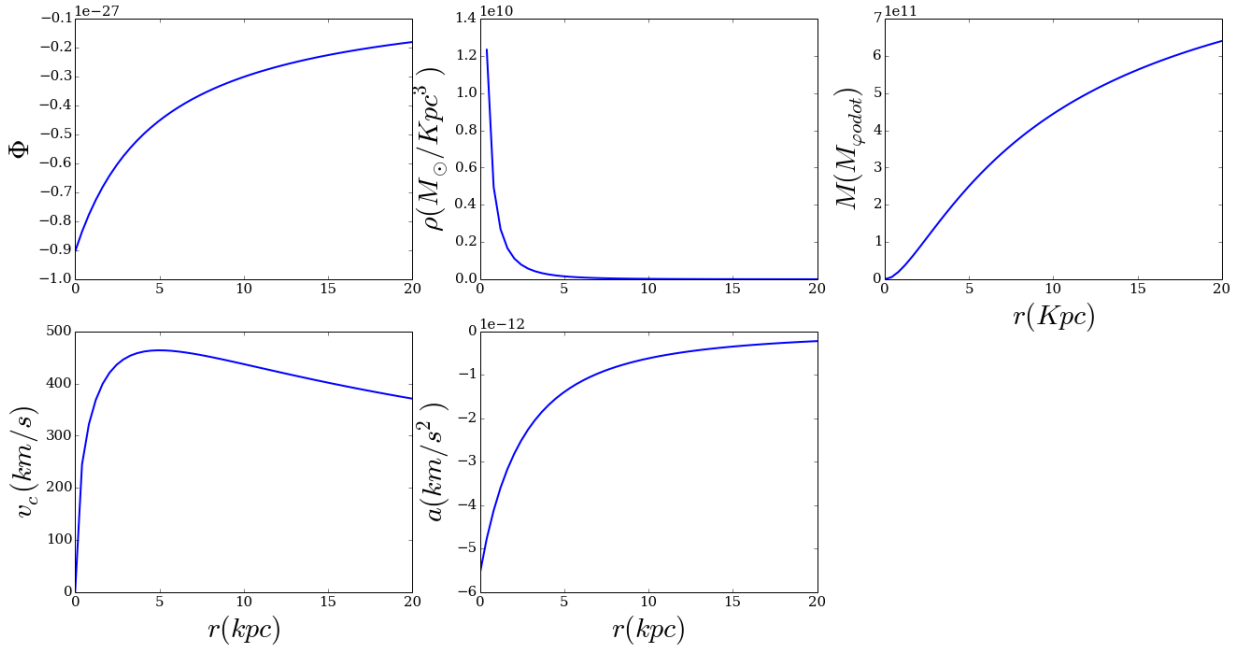


## 2.3 Singular Isothermal Sphere

The Singular Isothermal Sphere (**SIS**) describes a system in which the particles follow a Maxwellian density distribution. With this distribution and the Poisson equation the follow density profiles could be derived.

$$\rho_{iso}(r) = \frac{\sigma^2}{2\pi G(r^2 + a^2)} \tag{24}$$

Following the same procedure as with the previuos profiles we find $M, \Phi$ and $v_c$.

$$M_{iso}(< r) = \frac{2\sigma(r + a)}{G} \tag{25}$$

$$\Phi_{iso}(r) = 2\sigma^2 ln(r + a) + const. \tag{26}$$

$$v_c(r) = \sqrt{2}\sigma \tag{27}$$

$$a = -\frac{v^2}{(r + a)} \tag{28}$$

This profile is quite different to the previous ones due to the fact that here the input is the velocity instead of the total Mass.

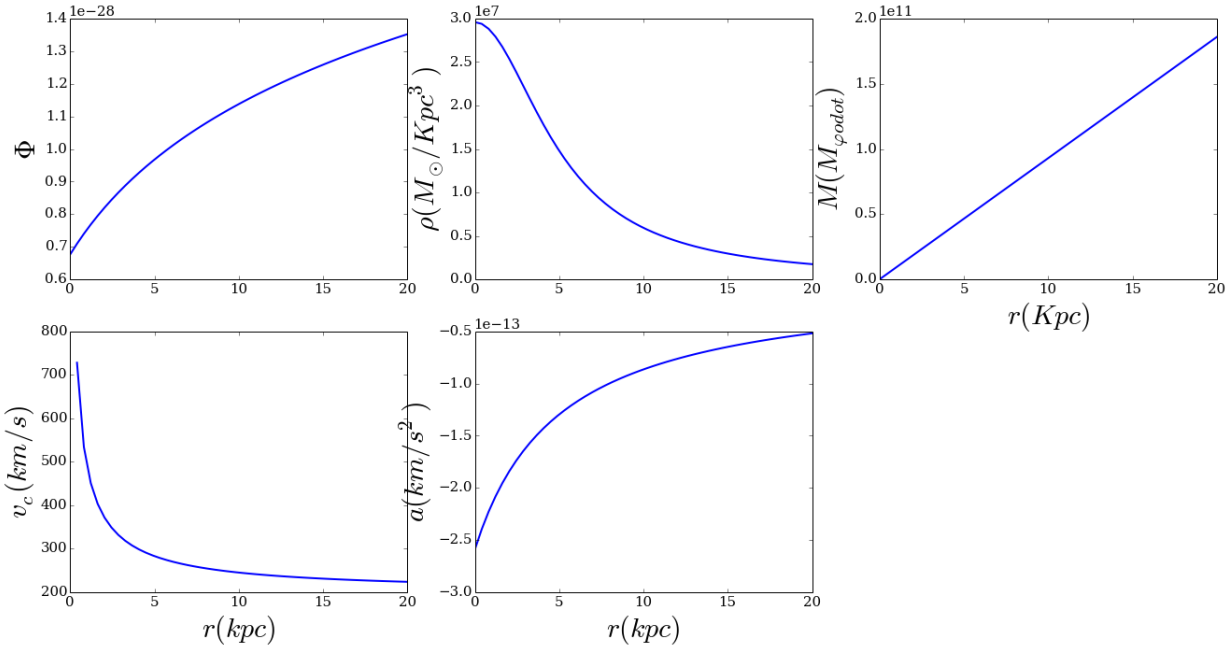


## 2.4 NFW

$$\rho_{NFW}(r) = \frac{M_{vir}}{2\pi a^3 (r/a)(1+r/a)^2} \tag{29}$$

$$M_{NFW}(r) = M_{vir} f(x)/f(c_{vir}) \tag{30}$$

Where $x = r/a$, is useful to define the function $f(x)$ as:

$$f(x) = ln(1+x) - \frac{x}{1+x} \tag{31}$$

Then 30 can be expresed as:

$$M_{NFW} = 4\pi\rho_a a^3 f(x) \tag{32}$$

$$\Phi_{NFW} = -4\pi G M \frac{ln(1+r/a)}{r} \tag{33}$$

$$c(M_{vir}) = 9.60 \left(\frac{M_{vir}}{10^{12} h^{-1} M_\odot}\right)^{-0.075} \tag{34}$$

$$v_c(r) = \sqrt{\left(\frac{M(r)G}{r}\right)} = \sqrt{\left(\frac{GM_{vir} f(x)/f(c_{vir})}{r}\right)} \tag{35}$$

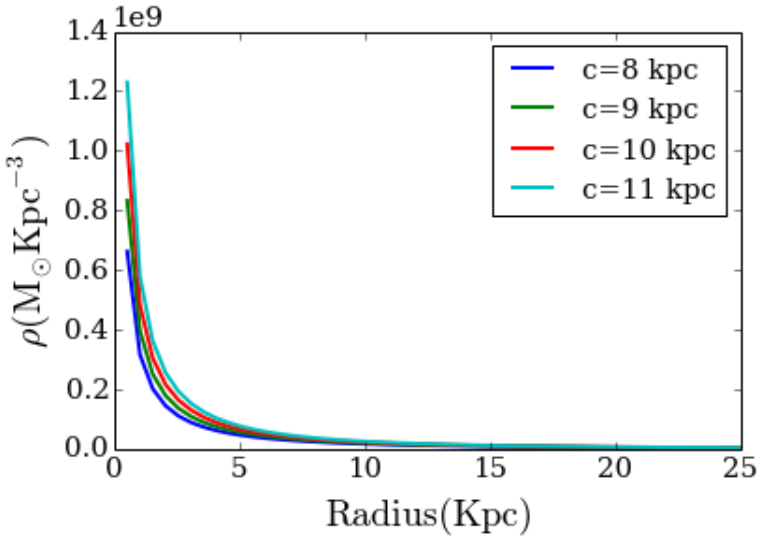
1e9
1.4
1.2
1.0
0.8
0.6
0.4
0.2
0.0
$\rho(M_\odot Kpc^{-3})$
0
5
10
15
20
25
Radius(Kpc)
c=8 kpc
c=9 kpc
c=10 kpc
c=11 kpc

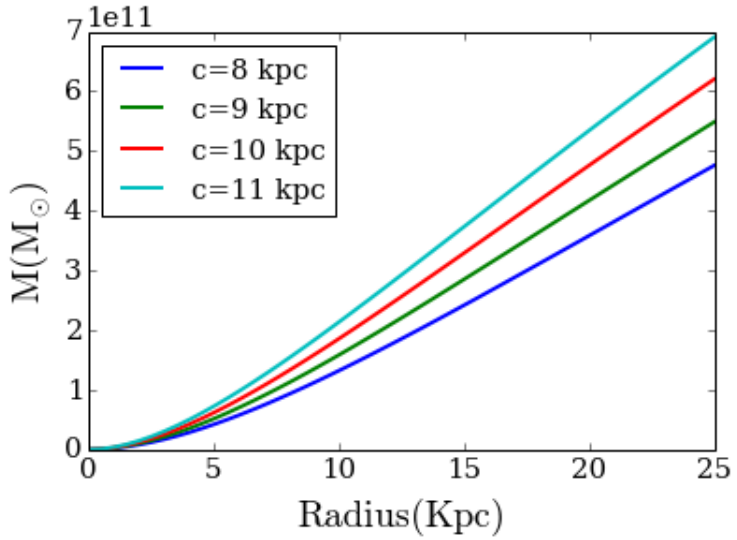
1e11
7
6
5
4
3
2
1
0
$M(M_\odot)$
0
5
10
15
20
25
Radius(Kpc)
c=8 kpc
c=9 kpc
c=10 kpc
c=11 kpc

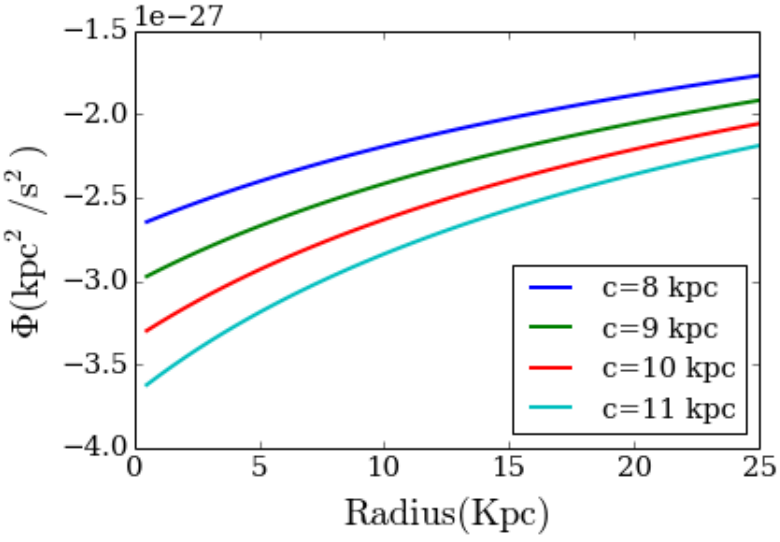
1e−27
−1.5
−2.0
−2.5
−3.0
−3.5
−4.0
$\Phi(kpc^2/s^2)$
0
5
10
15
20
25
Radius(Kpc)
c=8 kpc
c=9 kpc
c=10 kpc
c=11 kpc

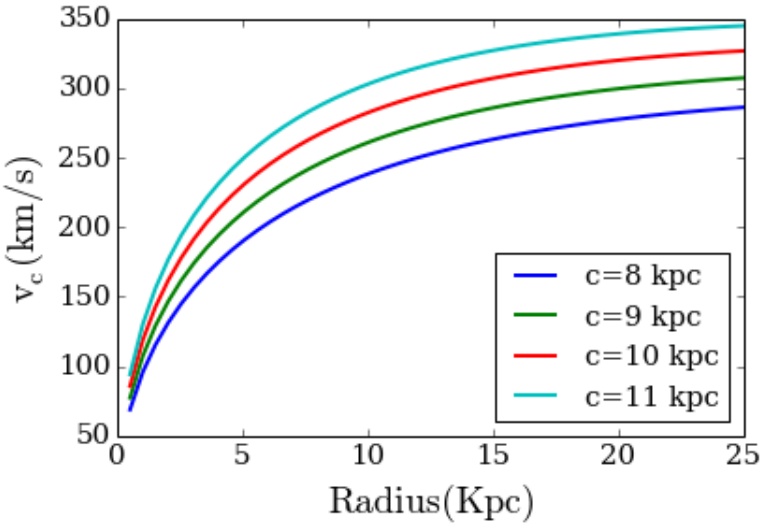


# 3 Conversion from NFW to the Hernquist profile

The average density of the NFW distribution can be expressed as:

$$\bar{\rho}_{NFW}(r) = \frac{3M_{NFW}(r)}{4\pi r^3} \tag{36}$$

And with eq.32 the $\bar{\rho_{NFW}}(r)$ takes de form:

$$\bar{\rho}_{NFW}(r) = 3\rho_a \left(\frac{a}{r}\right)^3 f(x) \tag{37}$$

Now if we want to find the relationship betwee $r_{200}$ and $r_{vir}$ for the NFW profile we have to apply eq8.

$$q = \frac{3\rho_a \frac{a}{r_{200}} f(c_{200})}{3\rho_a \frac{a}{r_{vir}} f(c)} = \frac{c_{200}^3 f(c_{200})}{c_{vir^3} f(c_{vir})} \tag{38}$$

$$\frac{c_{200}}{c_{vir}} = \left(\frac{f(c_{200})}{q f(c_{vir})}\right)^{1/3} \tag{39}$$

For $c_{vir} = 10$ this function is shown in Fig.??, where $y = \frac{c_{200}}{c_{vir}} - \left(\frac{f(c_{200})}{q f(c_{vir})}\right)^{1/3}$

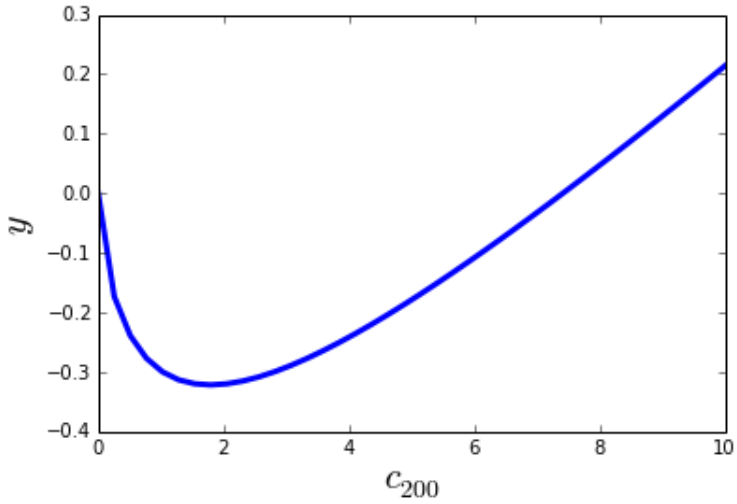


Note that the solution of Eq.39 is when $y = 0$, one solution is $c_{200} = 0$ but this is not of particular interest for us.

The other solution is computed analytically using the bisection algorithm. $c_{200} = 7.4$

In order to seek the equivalence between the NFW and the Hernquist profile, We have to match the same enclosed mass of both profiles at a given radius. To his end we have to find $M_H$ in terms of $r_s$.

$$M_H(r) = M_{NFW}(r) \tag{40}$$

$$\frac{M_H r^2}{a^2 + r^2} = 4\pi\rho_s r_s^3 \left[ Ln(1+x) - \frac{x}{1+x} \right] \tag{41}$$

In the limit $r \to 0$

$$M_H = \frac{4\pi\rho_s r_s^3 a^2}{r^2} \left[ (x - \frac{x^2}{2}) - x \right] \tag{42}$$

$$M_H = 4\pi\rho_s r_s^3 \frac{a^2}{r^2} \left( -\frac{r^2}{2r_s^2} \right) \tag{43}$$

$$M_H = 2\pi r_s a^2 \tag{44}$$

With this relation is possible now to match both profiles at a given radius $\tilde{r}$

$$M_H(\tilde{r}) = M_{NFW}(\tilde{r}) \tag{45}$$

$$2\pi\rho_s a^2 r_s \frac{\tilde{r}^2}{a^2} \frac{1}{\left(1 + \frac{\tilde{r}}{a}\right)^2} = 4\pi\rho_s r_s^3 \left( Ln\left(1 + \frac{\tilde{r}}{r_s}\right) - \frac{\tilde{r}}{\tilde{r} + r_s} \right) \tag{46}$$

$$\frac{\tilde{r}^2 a^2}{(a+\tilde{r})^2} = 2r_s^2 \left( Ln\left(1 + \frac{\tilde{r}}{r_s}\right) - \frac{\tilde{r}}{\tilde{r} + r_s} \right) \tag{47}$$

$$\frac{\tilde{r}^2 a^2}{(a+\tilde{r})^2} = 2r_s^2 f(\tilde{x}) \tag{48}$$

$$\left(\frac{a}{r_s}\right)^2 = \frac{2}{\tilde{r}^2}(a+\tilde{r})^2 f(\tilde{x}) \tag{49}$$

$$\frac{a}{r_s} = \frac{[2f(\tilde{x})]^{1/2}}{\tilde{r}}(a+\tilde{r}) \tag{50}$$

$$\left(\frac{a}{r_s}\right)\left(1 - \frac{[2f(\tilde{x})]^{1/2}}{\tilde{x}}\right) = [2f(\tilde{x})]^{1/2} \tag{51}$$

$$\frac{a}{r_s} = \frac{[2f(\tilde{x})]^{1/2}}{\left(1 - \frac{[2f(\tilde{x})]^{1/2}}{\tilde{x}}\right)} \tag{52}$$

$$\frac{a}{r_s} = \frac{[2f(\tilde{x})]^{1/2}\tilde{x}}{\tilde{x} - (2f(\tilde{x})^{1/2})} = \frac{1}{\left([2f(\tilde{x})]^{-1/2} - \frac{1}{\tilde{x}}\right)} \tag{53}$$

Finally the ratio of the enclosed mass of the Hernquist and the NFW profiles is:

$$\frac{M_H}{M_{vir}} = \frac{2\pi\rho_s a^2 r_s}{4\pi\rho_s r_s^3 f(c_{vir})} = \frac{1}{2f(c_{vir})}\left(\frac{a}{r_s}\right)^2 \tag{54}$$

Discs

# 4 Disc Potentials

## 4.1 Miyamoto-Nagai potential

For describing discs potentials it is better to change to cylindrical coordinates (R, z, $\phi$). The most known and used profile is the Miyamoto-Nagai profile [Miyamoto and Nagai, 1975].

$$\Phi_M(R,z) = -\frac{GM}{\sqrt{R^2 + (a + \sqrt{(z^2+b^2)})^2}} \tag{55}$$

$$\rho_M(R,Z) = \left(\frac{b^2 M}{4\pi}\right)\frac{aR^2 + (a+3\sqrt{z^2+b^2})(a+\sqrt{z^2+b^2})^2}{[R^2 + (a^2 + \sqrt{z^2+b^2})^2]^{5/2}(z^2+b^2)^{3/2}} \tag{56}$$

$$v_c = \sqrt{\frac{GMR}{(R^2 + (a+\sqrt{z^2+b^2})^2)^{3/2}}} \tag{57}$$

$$M(r) = \frac{v_c^2 r}{G} \tag{58}$$

$$M(<r) = \frac{MR^3}{(R^2 + (a + \sqrt{z^2 + b^2})^2)^{3/2}} \tag{59}$$

$$\vec{a} = \frac{-GMR}{(R^2 + (a + \sqrt{z^2 + b^2})^2)^{3/2}}\hat{\mathbf{R}} - \frac{GMz(a + \sqrt{z^2 + b^2})}{(R^2 + (a + \sqrt{z^2 + b^2})^2)^{3/2}\sqrt{z^2 + b^2}}\hat{\mathbf{z}} \tag{60}$$

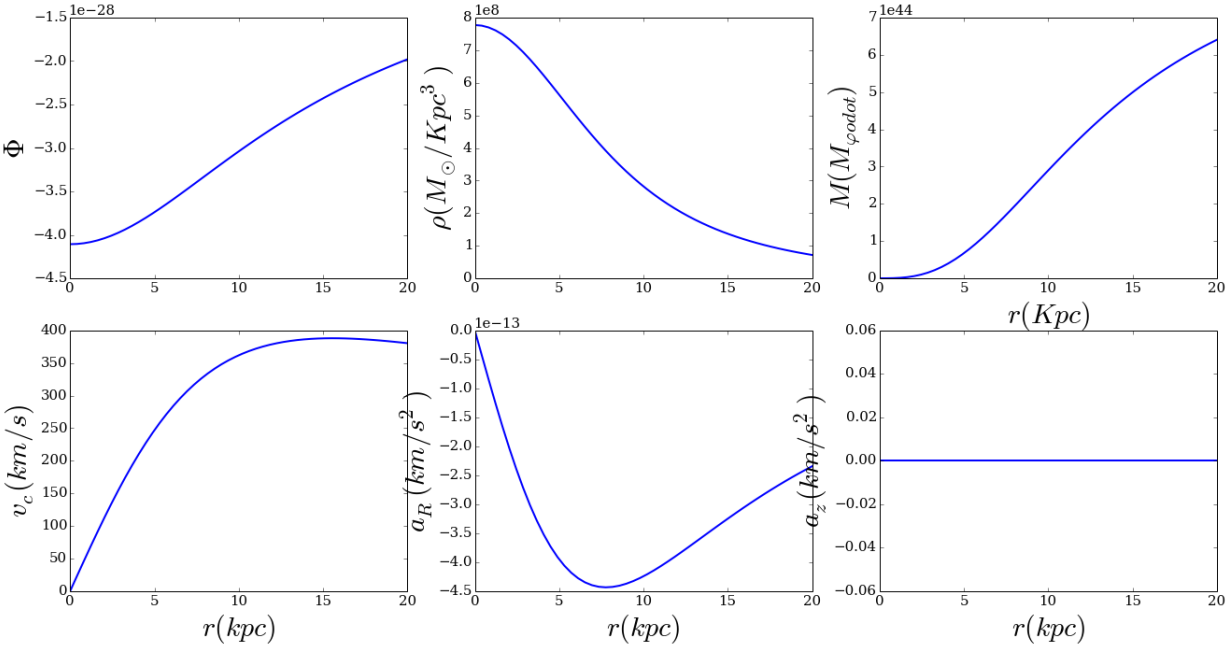

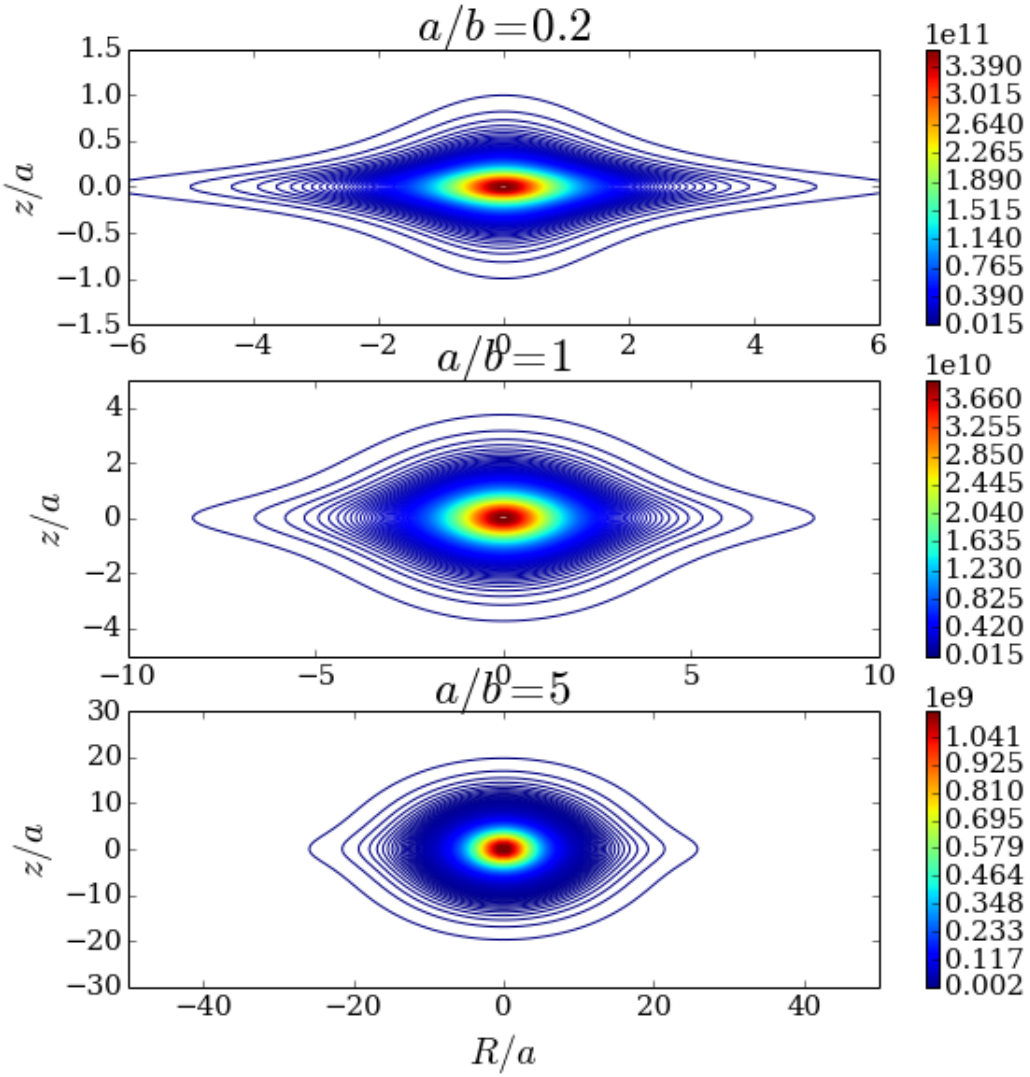


# 5 Logarithmic Profile

$$\Phi_L(R,z) = \frac{1}{2}v_0^2 ln\left(R_c^2 + R^2 + \frac{z^2}{q_\phi^2}\right) + constant \tag{61}$$

The circular velocity is $v_c^2(R,z) = R\frac{d\Phi}{dR}$:

$$v_c(R,z=0) = \sqrt{R\frac{d\Phi_L}{dr}} = \frac{v_0 R}{\sqrt{R_c^2 + R^2 + z^2/q_\phi^2}} \tag{62}$$

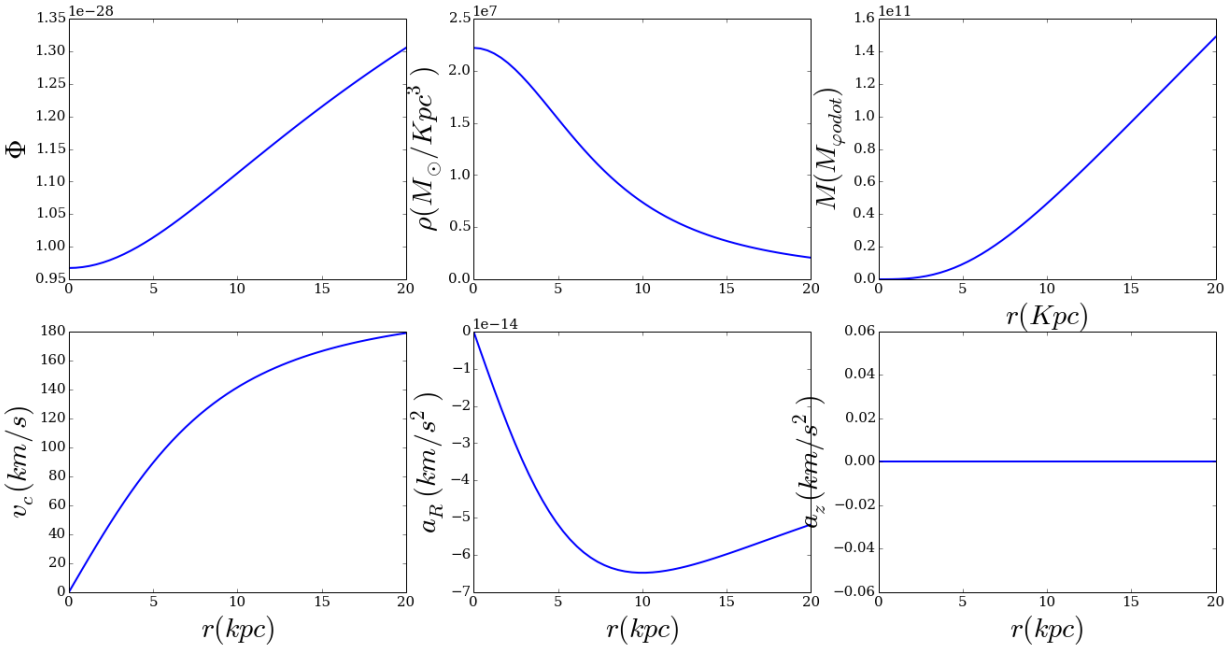


$$M(<R) = \frac{v_0^2 R^3}{G(R_c^2 + R^2 + z^2/q_\phi^2)} \tag{63}$$

To derive the density we make use of Poisson's equation in cylindrical coordinates:

$$\rho_L(R,z) = \frac{\nabla^2 \Phi_L}{4\pi G} = \frac{1}{4\pi G}\left(\frac{1}{r}\frac{d}{dR}R\frac{d}{dR} + \frac{d^2}{dz^2}\right)\Phi_L \tag{64}$$

$$\rho_L(R,z) = \frac{v_0^2}{8\pi G}\left(\frac{1}{R}\frac{4R(R_c^2 + R^2 + \frac{z^2}{q_\phi^2}) - 4R^3}{(R_c^2 + R^2 + \frac{z^2}{q_\phi^2})^2} + \frac{\frac{2}{q_\phi^2}(R_c^2 + R^2 + \frac{z^2}{q_\phi^2}) - \frac{4z^2}{q_\phi^4}}{(R_c^2 + R^2 + \frac{z^2}{q_\phi^2})^2}\right) \tag{65}$$

$$\rho_L(R,z) = \frac{v_0^2}{4\pi G q_\phi^2}\frac{(2q_\phi^2 + 1)R_c^2 + r^2 + (2 - q_{\Phi^2})z^2}{(R_c^2 + r^2 + z^2 q_\Phi^{-2})^2} \tag{66}$$

$$a = -\frac{v_0^2}{(R_c^2 + R^2 + z^2/q_\phi^2)}(R\hat{\mathbf{R}} + z/q_\phi^2\hat{\mathbf{z}}) \tag{67}$$

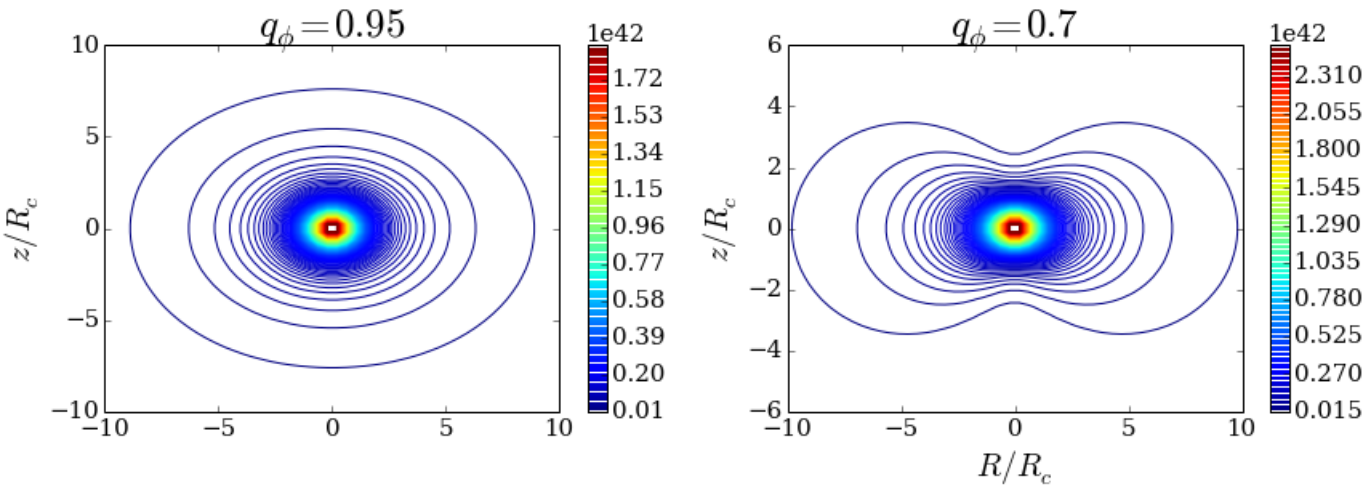


Triaxial

# 6 Triaxial Potentials

## 6.1 Logarithmic Triaxial Density Profile

Motivated by the fact that the models of the Milky Way Dark Matter halo at that time can not reproduce the Sgr stream. Mainly because in axisietric potentials it is not possible to fit the angular precession and the the distance of the stream. Law et al. [2009] propose a triaxial halo Eq.68 which is also in agreement with the CDM paradigm that predicts triaxial halos rather than spherical Lee and Suto [2003]. Law et al. [2009] report results of the orbital integration in which they find that the best fit in their triaxial halo is for $q_z = 1.25$, $q_1 = 1.5$ and $\phi = 90$. Law and Majewski [2010] made N-body simulations in which they include the triaxial halo potential.

$$\Phi = v_{halo}^2 ln(C_1 x^2 + C_2 y^2 + C_3 xy + (z/q_z)^2 + r_{halo}^2) \tag{68}$$

Where the constants $C_1, C_2, C_3$ are defined as:

$$C_1 = \left( \frac{cos^2\phi}{q_1^2} + \frac{sin^2\phi}{q_2^2} \right) \tag{69}$$

$$C_2 = \left( \frac{cos^2\phi}{q_2^2} + \frac{sin^2\phi}{q_1^2} \right) \tag{70}$$

$$C_3 = 2sin\phi cos\phi \left( \frac{1}{q_1^2} - \frac{1}{q_2^2} \right) \tag{71}$$

From Eq.68 we can derive the circular velocity $v_c$.

$$v_c^2 = r\nabla\Phi \tag{72}$$

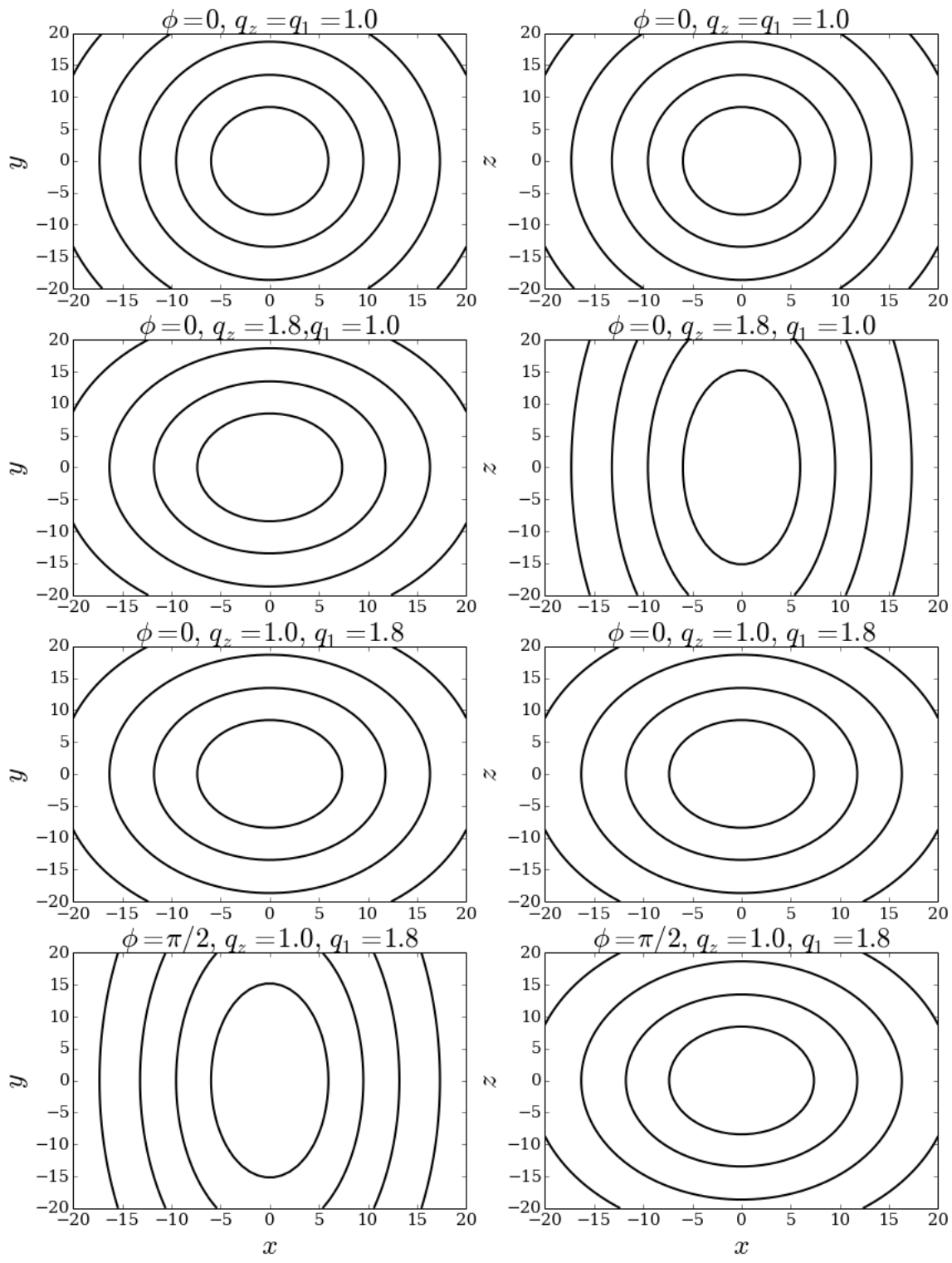


Figure 2: Logarithmic Triaxial Potential. In the top panel

$$\nabla\Phi = \frac{d}{dx}\Phi\hat{i} + \frac{d}{dy}\Phi\hat{j} + \frac{d}{dz}\Phi\hat{k} \tag{73}$$

$$\nabla\phi = v_{halo}^2 \left( \frac{(2C_1x + C_3y)\hat{i} + (2C_2y + C_3x)\hat{j} + (2z/q_z^2)\hat{k}}{(C_1x^2 + C_2y^2 + C_3xy + (z/q_z)^2 + r_{halo}^2)} \right) \tag{74}$$

$$v_c = v_{halo}\sqrt{\frac{r((2C_1x + C_3y)^2 + (2C_2y + C_3x)^2 + (2z/q_z^2)^2)^{1/2}}{(C_1x^2 + C_2y^2 + C_3xy + (z/q_z)^2 + r_{halo}^2)}} \tag{75}$$

$$a = -v_{halo}^2 \left( \frac{(2C_1x + C_3y)\hat{i} + (2C_2y + C_3x)\hat{j} + (2z/q_z^2)\hat{k}}{(C_1x^2 + C_2y^2 + C_3xy + (z/q_z)^2 + r_{halo}^2)} \right) \tag{76}$$

$$M(< R) = \frac{v_{halo}^2 r^2}{G} \frac{((2C_1x + C_3y)^2 + (2C_2y + C_3x)^2 + (2z/q_z^2)^2)^{1/2}}{(C_1x^2 + C_2y^2 + C_3xy + (z/q_z)^2 + r_{halo}^2)} \tag{77}$$

[Law and Majewski, 2010] fixed the value of $v_{halo}$ in order that the MW rotation curve reproduce the obervsed value of $v_{LSR} = 220km/s$ at $R_\odot$ this implies that $v_{halo} = 135km/s$. The rotation curve of is presented in Fig.**??**, the MW rotation curve is also presented in Fig.**??** all the paremeters of this rotation curve are summarized in Table**??**.

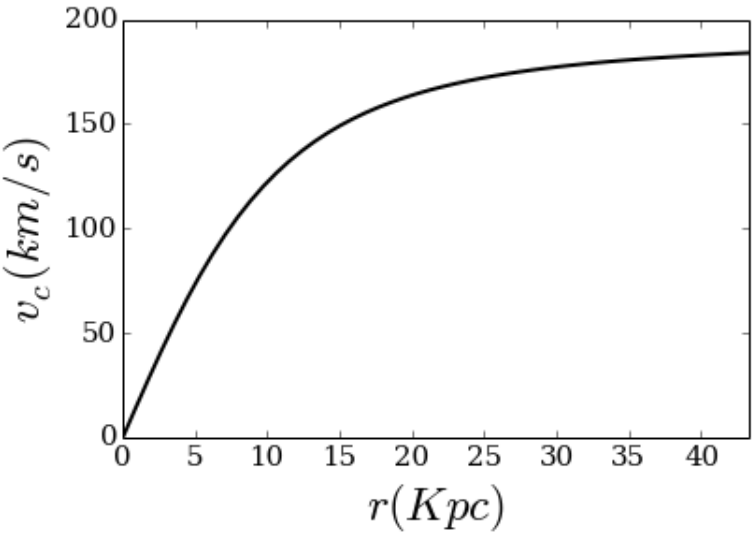

# 7 Modelling the MW

| Component | Besla07 | LM2010 | Roeland12 | Vera-Helmi13 |
|---|---|---|---|---|
| Disk Model | Miyamoto-Nagai | Miyamoto-Nagai | | Miyamoto-Nagai |
| Disk Mass($M_\odot$) | $5.5^{10}$ | $1.0 \times 10^{11}$ | | $1.0 \times 10^{11}$ |
| Disk Param | $R_d = 3.5, z = r_{disk}/5.0$ | $\alpha = 1, a = 6.5kpc, b = 0.6kpc$ | | $, a = 6.5kpc, b = 0.26Kpc$ |
| Bulge Model | Hernquist | Hernquist | | Hernquist |
| Bulge Mass($M_\odot$) | $10^{10}$ | $3.4 \times 10^{10}$ | | $3.4 \times 10^{11}$ |
| Bulge Param | $0.6kpc$ | $c = 0.7kpc$ | $0.6Kpc$ | $0.7Kpc$ |
| DM halo Model | NFW | Triaxial 6.1 | Hernquist(NFW) | Triaxial-Oblate |
| DM halo mass($M_\odot$) | $10^{12}$ | $\times 1.5 \times 10^{12}$ | $10^12$ | |
| Solar Velocity | | | 239 | 225.2 |
| Halo Param | $c = 11, r_{vir} = 258Kpc$ | $r_{halo} = 12Kpc$ | | $d = 12kpc, q_z = 0.9, q_1 = 1.38$ $q_2 = 1, q_3 = 1.36, \phi = 97, r_a = 30kpc$ |
| Solar distance $R_\odot$ (kpc) | 8.0 | 8.0 | | 8.0 |
| reference | Besla07 | LM2010 | | Vera13 |

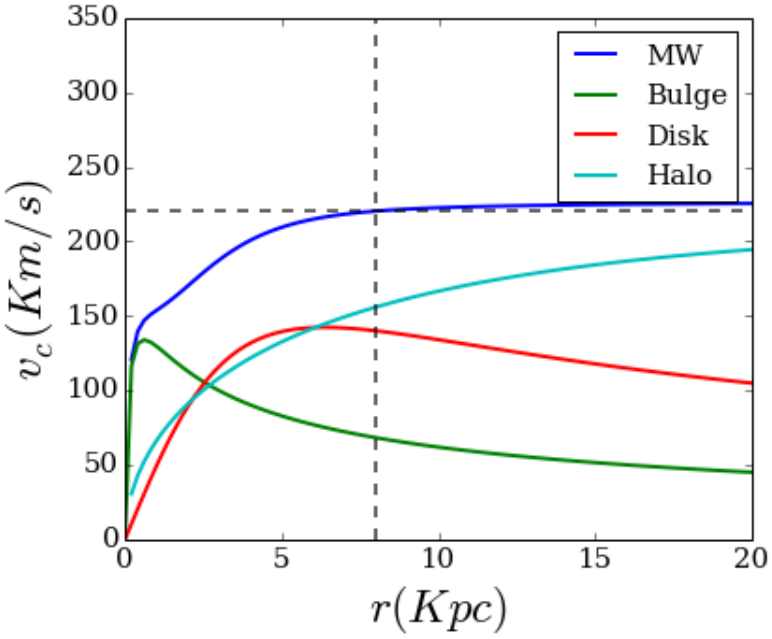

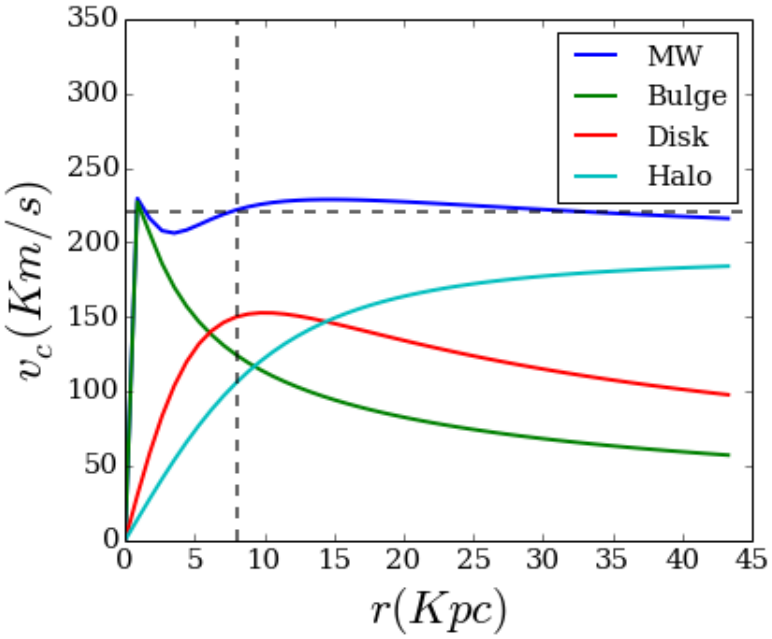


## 7.1 Vera-Ciro & Helmi models

[**?**] study a dark matter halo that is oblate in the center and triaxial in the outskirts. The motivations are that the disk is expected to modify the inner halo shape towards an oblate also if the halo is oblate at the inner the disk stability is ensured. They argue that the triaxial halo configuration of [Law and Majewski, 2010] it's not common in the LCDM model due to the small c/a ratio compared to LCDM predictions.

They integrate orbits of tests particles in the potential Eq.**??** for a period of 2gyr backwards and forward. For every test particle they select 10 random times in the orbit of this test particle from which they have positions and velocities. With this methodology they reproduce observables that might be compared with the Sgr stream.

The results from this numerical experiment is that they have a good fit in some parts of the orbits see Fig.2 of that paper and that the fit does not depend strongly in the parameter $r_a$ in the halo potential.

In the second part of this paper they study the effect of torques in the Sgr stream. The authors argue that there are two torques, one from the triaxality of the halo itself and other one due to the LMC. Interestingly the mayor axis of the triaxial potential in [Law and Majewski, 2010] is in the direction towards the LMC. They studied the magnitude of both torques and they found that both have equally effect in the Sgr stream.

As a result they modify the parameters of the halo model in order to account for the additional torque of the LMC, these new parameters are now more consistent with those expected from the LCDM model. For the orbit integration they also take into account the potential of the LMC. With these considerations they fit better the Sgr stream see Fig.5 of that paper.

$$\Phi_s(r) = v_{halo}^2 ln(\tilde{r}^2 + d^2) \tag{78}$$

$$\tilde{r} = \frac{r_a + t_T}{r_a + r_A} r_A \tag{79}$$

$$r_A^2 = x^2 + y^2 + \frac{z^2}{{q_z}^2} \tag{80}$$

$$r_T^2 = C_1 x^2 + C_2 y^2 + C_3 xy + \frac{z^2}{q_3^2} \tag{81}$$

Where $C_1, C_2, C_3$ are the same as in the triaxial model.

### 7.1.1 Acceleration

Then the acceleration would be:

$$a = -\nabla\Phi \tag{82}$$

$$-\nabla\Phi = -v_{halo}^2 \frac{2\tilde{r}}{(\tilde{r}^2 + d^2)} \left( \frac{d\tilde{r}}{dx}\hat{i} + \frac{d\tilde{r}}{dy}\hat{j} + \frac{d\tilde{r}}{dz}\hat{k} \right) \tag{83}$$

To evaluate this derivatives the following expressions are useful:

$$\frac{\partial r_T}{\partial x} = \frac{C_1 x + C_3 y/2}{(C_1 X^2 + C_2 y^2 + C_3 xy + z^2/q_3^2)^{1/2}} \tag{84}$$

$$\frac{\partial r_T}{\partial y} = \frac{C_2 y + C_3 x/2}{(C_1 X^2 + C_2 y^2 + C_3 xy + z^2/q_3^2)^{1/2}} \tag{85}$$

$$\frac{\partial r_T}{\partial z} = \frac{z/q_3^2}{(C_1 X^2 + C_2 y^2 + C_3 xy + z^2/q_3^2)^{1/2}} \tag{86}$$

$$\frac{\partial r_A}{\partial x} = \frac{x}{(x^2 + y^2 + z^2/{q_z}^2)^{1/2}} \tag{87}$$

$$\frac{\partial r_A}{\partial y} = \frac{y}{(x^2 + y^2 + z^2/{q_z}^2)^{1/2}} \tag{88}$$

$$\frac{\partial r_A}{\partial z} = \frac{z/q_z^2}{(x^2 + y^2 + z^2/{q_z}^2)^{1/2}} \tag{89}$$

$$\frac{\partial \tilde{r}}{\partial \alpha} = \frac{\left( \frac{dr_T}{d\alpha} r_A + r_T \frac{dr_A}{d\alpha} \right)(r_a + r_A) - (r_a + r_T) r_A \frac{dr_A}{d\alpha}}{(r_a + r_A)^2} \tag{90}$$

Where $\alpha$ stands for the $x, y, z$
With these definitions the acceleration terms are:

$$a_x = -\frac{v_{halo}^2 2\tilde{r}}{(\tilde{r}^2 + d^2)} \frac{\partial \tilde{r}}{\partial x} \tag{91}$$

$$a_y = -\frac{v_{halo}^2 2\tilde{r}}{(\tilde{r}^2 + d^2)} \frac{\partial \tilde{r}}{\partial y} \tag{92}$$

$$a_z = -\frac{v_{halo}^2 2\tilde{r}}{(\tilde{r}^2 + d^2)} \frac{\partial \tilde{r}}{\partial z} \tag{93}$$

### 7.1.2 Circular velocity

$$v_c{}^2 = r|-\nabla\phi| = -\frac{2\tilde{r}^2 v_{halo}^2}{\tilde{r}^2 + d^2} \left( \left(\frac{d\tilde{r}}{dx}\right)^2 + \left(\frac{d\tilde{r}}{dy}\right)^2 + \left(\frac{d\tilde{r}}{dz}\right)^2 \right)^{1/2} \tag{94}$$

# 8 code

Running GalIC on el Gato:
go to `ICs/GalIC` then charge `gsl` and `intel-mpi` modules and then run `bsub < galic.sh`

# 9 TO-DO:

- One big figure per profile
- Put all the acceleration terms
- Vera-Ciro model
- Rotation curves of the MW for all the models
- NFW HErnquist plot equivalence
- note: Klypin relation between $c$ and $M_{vir}$ Doesn't take into account adiabatic contraction.
- work in the code that integrates the orbits using the accelerations. (Viernes)

# References


J. Binney and S. Tremaine. *Galactic Dynamics: Second Edition*. Princeton University Press, 2008.

V. R. Eke, S. Cole, and C. S. Frenk. Cluster evolution as a diagnostic for Omega. , 282: 263–280, September 1996.

G. L. Bryan and M. L. Norman. Statistical Properties of X-Ray Clusters: Analytic and Numerical Comparisons. , 495:80–99, March 1998. doi: 10.1086/305262.

M. Miyamoto and R. Nagai. Three-dimensional models for the distribution of mass in galaxies. , 27:533–543, 1975.

D. R. Law, S. R. Majewski, and K. V. Johnston. Evidence for a Triaxial Milky Way Dark Matter Halo from the Sagittarius Stellar Tidal Stream. , 703:L67–L71, September 2009. doi: 10.1088/0004-637X/703/1/L67.

J. Lee and Y. Suto. Modeling Intracluster Gas in Triaxial Dark Halos: An Analytic Approach. , 585:151–160, March 2003. doi: 10.1086/345931.

D. R. Law and S. R. Majewski. The Sagittarius Dwarf Galaxy: A Model for Evolution in a Triaxial Milky Way Halo. , 714:229–254, May 2010. doi: 10.1088/0004-637X/714/1/229.